

DETECTION OF DARK MATTER CONCENTRATIONS IN THE FIELD OF CL 1604+4304 BY WEAK LENSING

K. UMETSU AND T. FUTAMASE

Astronomical Institute, Tohoku University, Sendai 980-8578, Japan
keiichi@astr.tohoku.ac.jp, tof@astr.tohoku.ac.jp

We present a weak-lensing analysis of a region around the galaxy cluster Cl 1604+4304 ($z = 0.897$) on the basis of the deep observations with the *Hubble Space Telescope* (*HST*)/Wide Field Planetary Camera 2 (WFPC2). We apply a variant of Schneider's aperture mass technique to the observed WFPC2 field and obtain the distribution of weak-lensing signal-to-noise ratio (S/N) within the field. The resulting S/N map reveals a clear pronounced peak located about 1.7 ($850h_{50}^{-1}$ kpc at $z = 0.897$) southwest of the second peak associated with the optical cluster center determined from the dynamical analysis of Postman et al. A non-linear finite-field inversion method has been used to reconstruct the projected mass distribution from the observed shear field. The reconstructed mass map shows a super-critical feature at the location of the S/N peak as well as in the cluster central region. Assuming the redshift distribution of field galaxies, we obtain the total mass in the observed field to be $1.0 \times 10^{15} h_{50}^{-1} M_{\odot}$ for $\langle z \rangle = 1.0$. The estimated mass within a circular aperture of radius $280h_{50}^{-1}$ kpc centered on the dark clump is $2.4 \times 10^{14} h_{50}^{-1} M_{\odot}$. We have confirmed the existence of the 'dark' mass concentration from another deep *HST* observation with a slightly different ($\sim 20''$) pointing.

1 Introduction

Weak shear fields of high-redshift galaxies are promising, efficient tools to investigate the mass distribution on cluster-supercluster scales^{2,4,5,8} and provide a unique mean to detect dark mass concentrations^{3,11}. Wide-field weak-lensing surveys of projected mass overdensities can probe the statistical clustering properties and underlying cosmology¹.

Recent observations⁷ have revealed the existence of a supercluster at a high redshift of $z \approx 0.9$. This supercluster contains two massive galaxy clusters, Cl 1604+4304 at $z = 0.897$ and Cl 1604+4321 at $z = 0.924$. The two clusters are separated by $17'$ on the sky, corresponding to a projected separation of $\sim 9h_{50}^{-1}$ Mpc. Cl 1604+4304 is located at $(\alpha_{J2000}, \delta_{J2000}) = (16^{\text{h}} 04^{\text{m}} 19.5^{\text{s}}, +43^{\circ} 04' 33.''9)$ and one of the optically-selected high-redshift cluster candidates studied by Oke, Postman, & Lubin⁹. Postman, Lubin, & Oke¹⁰ presented a detailed photometric and spectroscopic survey of the cluster and obtained a velocity dispersion of 1226 km s⁻¹ and a dynamical mass estimate of $6.2 \times 10^{15} h_{50}^{-1} M_{\odot}$.

Here, we present a weak lensing analysis of the Cl 1604+4304 field on the basis of deep images taken with the *Hubble Space Telescope* (*HST*)/Wide Field Planetary Camera 2 (WFPC2). Throughout this paper, we will assume $\Omega_0 = 1$, $\Omega_{\Lambda} = 0$, and $H_0 = 50h_{50}$ km s⁻¹ Mpc⁻¹; $1'$ on the sky corresponds to $0.52h_{50}^{-1}$ Mpc at the cluster redshift.

2 *HST* observations and background galaxy catalogs

The cluster Cl 1604+4304 field was observed in 1994 and 1995 using the WFPC2 camera with the F814W filter on board the *HST* (P.I.: J. Westphal; proposal 5234). We retrieved the calibrated data for Cl 1604+4304 field from the *HST* archive. Both the 1994 and 1995 observations have the same total exposure time of 32 ksec, consisting of 16 single orbits of 2 ksec. The 1995 pointing covers the central region of Cl 1604+4304⁶, while the 1994 pointing is about $20''$ offset ($\Delta X \simeq 0.''1, \Delta Y \simeq 18.''2$) from the 1995 pointing. For this reason, Lubin et al. discarded the 1994 data from their analysis. We analyze both the 1994 and 1995 data separately. The PC chip was discarded from our analysis because of its brighter isophotal limit, so that the final

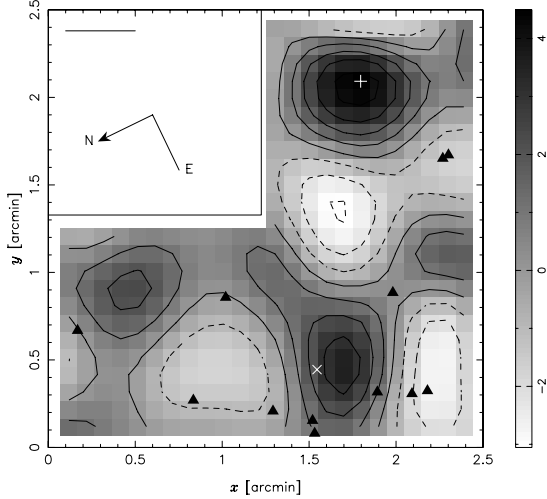


Figure 1: Contour plot of the weak-lensing S/N distribution in the 1995 data field. The solid and dashed lines indicate the positive and negative ones, respectively. The contours are stepped in units of 1. The filtering scale (0.4) used for the aperture mass measure is marked and the position of the dynamical cluster center is indicated (*cross*). The locations of 12 spectroscopically-confirmed cluster member galaxies are marked with triangle. The location of the first maximum is marked with a plus sign. The location of the second maximum coincides well with the dynamical center.

frame for each observation consists of three WFC chips. The side length of the WFPC2 field is about 2.5 ($1.26h_{50}^{-1}$ Mpc at $z = 0.897$). The detection and selection procedure leads to the final faint galaxy catalogs with total numbers of $N_g = 200$ and 241 , corresponding number densities of $n_g = 45.8$ and 56.8 arcmin $^{-2}$, for the 1994 and 1995 data, respectively (details are described in the original paper⁴⁴).

3 Weak lensing analysis of Cl 1604+4304

Since the 1995 pointing covers the central cluster region where a dynamical analysis was performed by Postman et al., we first analyzed the 1995 data. We measured the local weak lensing S/N $\nu(\vec{\theta}; \vartheta)$ with filtering radius $\vartheta = 0.4$ ($150h_{50}^{-1}$ kpc) on 24×24 grid points (except on the PC chip). Here $\nu(\vec{\theta}; \vartheta)$ is defined by

$$\nu(\vec{\theta}; \vartheta) := \frac{\sqrt{2} \sum_m p(|\vec{\theta} - \vec{\theta}_m|; \vartheta) \epsilon_t(\vec{\theta}_m; \vec{\theta})}{\sigma_\epsilon \sqrt{\sum_m p^2(|\vec{\theta} - \vec{\theta}_m|; \vartheta)}}, \quad (1)$$

where ϵ_t is the tangential component of the complex image ellipticity ϵ defined by $\epsilon_t(\vec{\theta}; \vec{\theta}_0) := -\Re[\epsilon(\vec{\theta})e^{-2i\phi}]$ with $\phi = \text{Arg}(\vec{\theta} - \vec{\theta}_0)$, σ_ϵ is the dispersion of the intrinsic source ellipticities, and $p(\theta; \vartheta) = W''(\theta; \vartheta) - W'(\theta; \vartheta)/\theta$ with $W(\theta; \vartheta)$ being a smooth, continuous window function having a characteristic scale of ϑ . In the present paper, we use a Gaussian window function of the form $W_G(\theta; \vartheta) = \exp(-\theta^2/\vartheta^2)/\pi\vartheta^2$, in which case $p(\theta; \vartheta) = 4(\theta/\vartheta)^2 \exp(-\theta^2/\vartheta^2)/\pi\vartheta^4 \equiv p_G(\theta; \vartheta)$.

Figure 1 displays the resulting weak-lensing S/N map obtained for the 1995 data. We find two S/N peaks above a threshold of $\nu_{\text{th}} = 3$. The first maximum has a peak height of $\nu = 4.5$ and its location is about 1.7 ($850h_{50}^{-1}$ kpc) southwest of the the optical cluster center (marked with cross) determined from the dynamical analysis⁴⁰. The peak height of the second maximum

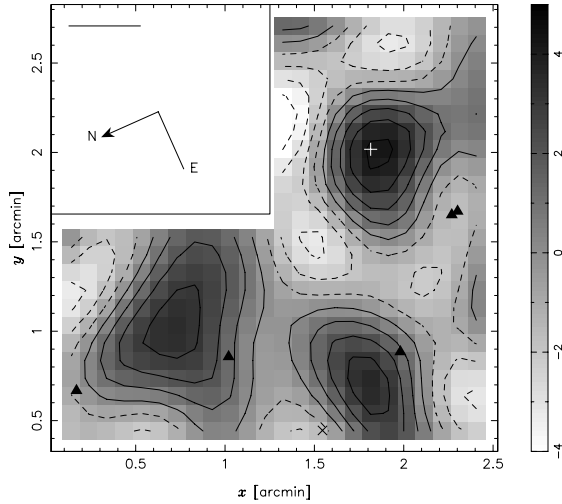


Figure 2: The same as Fig. 1 but obtained using the 1994 data. The same coordinate system as in Fig. 1 is used.

is $\nu = 3.6$ and located in the vicinity of the dynamical cluster center. This offset is about $0.'15$ ($75h_{50}^{-1}$ kpc) and comparable to the grid spacing of $0.'1$ ($50h_{50}^{-1}$ kpc), so that the second peak is consistent with the dynamical cluster center and associated with the cluster member galaxies⁶. In this field, there are a total of 12 cluster members whose redshifts are spectroscopically confirmed by Keck observations⁶. However, no cluster members are observed at around the first S/N peak because objects located on the upper edge of the WF4 chip (upper-right WF chip) are not contained within the sampled region of spectroscopic observations¹⁰.

Although the detection of the mass concentration cannot be confirmed spectroscopically from the available data, we have checked the stability and reliability of S/N maps. We find that the main features, i.e. the locations and heights of the peaks, are insensitive to the choice of the weight function or filtering scale. It should be noted that these main features are stable even if objects with large ellipticities ($|\epsilon| \geq 0.4$) are removed from our galaxy catalog, in which case the peak heights of the first and second maxima are 3.7 and 3.0, respectively. There still remains a possibility that the detected S/N peaks might be noise peaks due to the intrinsic source ellipticities or the anisotropic PSF. Van Waerbeke¹⁶ has shown from the simulated data that the probability distribution of the noise peaks in mass maps deviates from Gaussian and the probability of finding high noise peaks increases owing to the boundary effects. Since the field-of-view of the *HST*/WFC is small and we adopt a constant filtering scale, the obtained S/N maps may be affected by boundary effects. We can investigate such possibilities using independent deep observation of this field. In Fig. 2, we show the weak-lensing S/N map obtained from the 1994 data. Here we have used the same filtering scale and grid spacing as for the 1995 data. Comparing Fig. 2 with Fig. 1, we see that the first maximum in the 1994 S/N map corresponds to that in the 1995 S/N map. The first maximum in the 1994 S/N map has a peak height of $\nu = 4.2$, whose location coincides well with that of the first maximum in the 1995 S/N map ($\alpha_{J2000} = 16\text{h } 04\text{m } 15.7\text{s}$ and $\delta_{J2000} = +43\text{ deg } 03' 47.''2$). The identification of the first S/N maximum from two-different pointing observations indicates that the S/N maximum does not originate from the anisotropic PSF. Moreover, since the first maximum in the 1994 S/N map is located at the center of the WF4 chip, the S/N measure at the first peak cannot be affected by boundary effects. These results confirm the detection of ‘dark’ mass concentration associated with the first S/N maximum.

We have performed a non-linear finite-field inversion method^{12,13,15} to reconstruct the projected mass distribution within the 1995 data field. We calculated the smoothed ellipticity $\langle \epsilon \rangle$ ($\vec{\theta}$) on 20×20 grid points (except on the PC chip) using $W_G(\theta; \vartheta)$ with $\vartheta = 0.'35$ ($176h_{50}^{-1}$ kpc). In

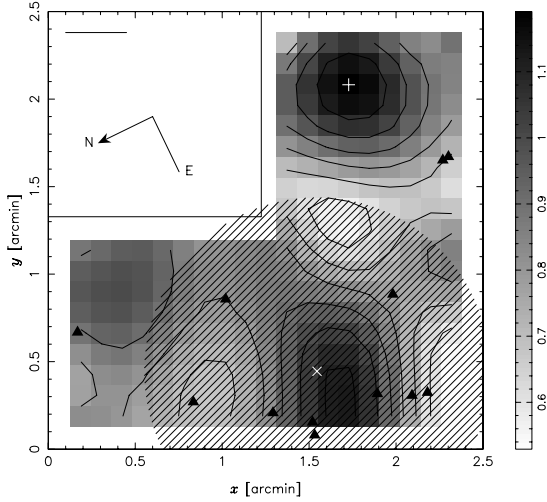


Figure 3: Contour plot of the κ_∞ -distribution reconstructed from the shear field of the 1995 observation. The contours are stepped in units of 0.1. The smoothing scale ($0.35''$) used to calculate the shear field is marked. The shaded area indicates the circular aperture of radius $500h_{50}^{-1}$ kpc centered on the dynamical cluster center (marked with \times). The side length is about $2.5''$ ($1.26h_{50}^{-1}$ Mpc at $z = 0.897$). The mass distribution is super-critical around the first maximum (marked with $+$) and the cluster central region.

Fig. 3, we show the reconstructed κ_∞ -map (κ_∞ is a convergence for sources at an infinite redshift) for a source redshift distribution $\langle z \rangle = 1.0$. In mass reconstruction, we implicitly assumed that the dark mass concentration has the same redshift $z = 0.897$ as Cl 1604+4304. We see from Figs. 1 and 3 that the local maxima in the S/N maps correspond to the mass peaks and that the weak-lensing S/N traces the projected mass, as expected. The κ_∞ -map shows a super-critical feature around the dark mass concentration ($\kappa_\infty = 1.19$) as well as in the cluster central region. The projected mass within the 1995 data field is obtained as $1.0 \times 10^{15} h_{50}^{-1} M_\odot$. From the mass map, the enclosed mass in a $280h_{50}^{-1}$ kpc radius centered on the dark mass concentration is calculated to be $2.4 \times 10^{14} h_{50}^{-1} M_\odot$: For the mass-to-light ratio, a lower limit is obtained as $M/L_B \approx 500h_{50}$ in solar units from an upperlimit on the dark clump's surface brightness.

4 Discussion and conclusions

We have performed a weak-lensing analysis on the deep images of a region around Cl 1604+4304 taken with the *HST*/WFPC2. We detected two significant maxima in the resulting weak-lensing S/N map: the second peak associated with the dynamical cluster center and the first peak located about $1.7''$ south of the dynamical center having no optical counter parts. The identification of high S/N peak from two-different pointing observations provides a robust evidence of dark mass concentration. Assuming that the dark mass clump has the same redshift as Cl 1604+4304, we reconstructed the projected mass distribution in the 1995 data field, from which we have estimated the mass within a circular aperture of radius $280h_{50}^{-1}$ kpc centered on the dark clump to be $2.4 \times 10^{14} h_{50}^{-1} M_\odot$. The obtained results indicate that this dark clump could be a compact, massive bound system associated with the supercluster at $z \approx 0.9$; the obtained mass will be overestimate if the redshift of the dark clump is much less than 0.897.

Our results demonstrate that the weak-lensing S/N statistics are powerful and efficient tools even for high-redshift cluster surveys ($z \sim 1$). For a further confirmation of the dark mass concentration, deep wide-field observations covering the entire supercluster field ($\sim 20''$) are required. Such observations can probe the mass distribution in the supercluster field extending over $\sim 10h_{50}^{-1}$ Mpc.

Acknowledgments

We are very grateful to the organizers for the exciting and interesting meeting. Part of this work is based on the observation with the NASA/ESA *Hubble space Telescope*, obtained from the data archive at the Space Telescope Science Institute (STScI). STScI is operated by the Association of Universities for Research in Astronomy, Inc. under the NASA contract NAS 5-26555.

References

1. Bahcall, N. A., Ostriker, J. P., Perlmutter, S., Steinhardt, P. J. 1999, *Sci* 284, 1481B
2. Bartelmann, M. & Schneider, P. 2000, *Phys. Rep.*, in press
3. Erben, T., Van Waerbeke, L., Mellier, Y., Schneider, P., Cuillandre, J.-C., Castander, F. J., & Dantel-Fort, M. 2000, *A&A*, 355, 23
4. Kaiser, N. & Squires, G. 1993, *ApJ*, 404, 441
5. Kaiser, N., Wilson, G., Luppino, G., Kofman, L., Gioia, I., Metzger, M., & Dahle, H. 1998, preprint astro-ph/9809268
6. Lubin, L., Postman, M., Oke, J. B., Ratnatunga, K. U., Gunn, J. E., Hoessel, J. G., & Schneider D. P. 1998, *ApJ*, 116, 584
7. Lubin, L., Brunner, R., Metzger, M. R., Postman, M., Oke, J. B. 2000, *ApJ*, 531, L5
8. Luppino, G. A. & Kaiser, N. 1997, *ApJ*, 475, 20
9. Oke, J. B., Postman, M., & Lubin, L. 1998, *ApJ*, 116, 549
10. Postman, M., Lubin, L., & Oke, J. B. 1998, *ApJ*, 116, 560
11. Schneider, P. 1996, *MNRAS*, 283, 837
12. Seitz, C. Kneib, J.-P., Schneider, P., & Seitz, S. 1996, *A&A*, 314, 707
13. Seitz, C. & Schneider, P. 1997, *A&A*, 318, 687
14. Umetsu, K. & Futamase, T. 2000, *ApJ*, 539, L5
15. Umetsu, K., Tada, M., & Futamase, T. 1999, *Prog. Theor. Phys. Suppl.*, 133, 53
16. Van Waerbeke, L. 2000, *MNRAS*, 313, 524